HHS Public Access

Author manuscript

Oncogene. Author manuscript; available in PMC 2016 November 28.

Published in final edited form as:

Oncogene. 2016 November 24; 35(47): 6077–6086. doi:10.1038/onc.2016.133.

Characterization of activating mutations of NOTCH3 in T cell acute lymphoblastic leukemia and anti-leukemic activity of NOTCH3 inhibitory antibodies

Paula Bernasconi-Elias[1], **Tiancen Hu**[1], **David Jenkins**[1,8], **Brant Firestone**[1], **Sara Gans**[1], **Esther Kurth**[1], **Paola Capodieci**[1], **Joelle Deplazes-Lauber**[2], **Konstantin Petropoulos**[2], **Phillip Thiel**[2,10], **Dirk Ponsel**[2,11], **Sung Hee Choi**[3,4], **Peter LeMotte**[1], **Anne London**[1], **Margaret Goetcshkes**[1,7], **Erin Nolin**[1], **Michael D. Jones**[1], **Kelly Slocum**[1], **Michael J. Kluk**[5,12], **David M. Weinstock**[3], **Alexandra Christodoulou**[3], **Olga Weinberg**[6], **Jan Jaehrling**[2], **Seth A. Ettenberg**[1,9], **Alan Buckler**[1,7], **Stephen C. Blacklow**[3,4,5], **Jon C. Aster**[4,5], and **Christy J. Fryer**[1]

[1]Novartis Institutes for Biomedical Research, Cambridge, Massachusetts

[2]MorphoSys AG, Martinsried, Germany

[3]Dana Farber Cancer Institute, Boston, MA

[4]Harvard Medical School, Boston, MA

[5]Brigham and Women's Hospital, Boston, MA

[6]Children Hospital Boston, Boston, MA

Abstract

Notch receptors have been implicated as oncogenic drivers in several cancers, the most notable example being NOTCH1 in T-cell acute lymphoblastic leukemia (T-ALL). To characterize the role of activated NOTCH3 in cancer, we generated an antibody that detects the neo-epitope created upon gamma-secretase cleavage of NOTCH3 to release its intracellular domain (ICD3), and sequenced the negative regulatory region (NRR) and PEST domain coding regions of NOTCH3 in a panel of cell lines. We also characterize NOTCH3 tumor-associated mutations that result in activation of signaling and report new inhibitory antibodies. We determined the structural basis for receptor inhibition by obtaining the first co-crystal structure of a NOTCH3 antibody with the NRR

Correspondence to Christy Fryer, Novartis Institutes for Biomedical Research, 250 Massachusetts Ave. Bldg 600-5B263, Cambridge, MA 02139. Tel: 617-871-4006. Fax: 617-871-7262, christy.fryer@novartis.com.

[7]present address: Biogen, Cambridge, MA

[8]present address: MedImmune, Gaithersburg, MD

[9]present address: Unum Therapeutics, Cambridge, MA

[10]present address: 1stQ Deutschland GmbH & Co KG, Mannheim, Germany

[11]present address: Roche AG, Penzberg, Germany

[12]present address: Cornell-Weill Medical College, New York, NY

Disclosure of Potential Conflicts of Interest: P. Bernasconi-Elias, T. Hu, B. Firestone, S. Gans, E. Kurth, P. Capodieci, P. LeMotte, A. London, E. Nolin, M. Jones, K. Slocum, are employees of Novartis Institutes for Biomedical Research. J. Deplazes-Lauber, K. Petropoulos, J. Jaehrling are employees of MorphoSys AG. S. Blacklow serves as a consultants for Novartis and receives research support through the Dana Farber - Novartis DDP. No other authors declare any conflicts of interest.

protein and defined two distinct epitopes for NRR antibodies. The antibodies exhibit potent anti-leukemic activity in cell lines and tumor xenografts harboring NOTCH3 activating mutations. Screening of primary T-ALL samples reveals that two of 40 tumors examined show active NOTCH3 signaling. We also identified evidence of NOTCH3 activation in 12 of 24 patient-derived orthotopic xenograft models, two of which exhibit activation of NOTCH3 without activation of NOTCH1. Our studies provide additional insights into NOTCH3 activation and offer a path forward for identification of cancers that are likely to respond to therapy with NOTCH3 selective inhibitory antibodies.

Keywords

Notch signaling; NOTCH3; T-ALL; inhibitory antibody

Introduction

Notch signaling regulates a diverse set of biological functions in developing embryos and adult tissues (1-3). In mammals, there are four Notch receptors (Notch1-4), which are all single-pass transmembrane proteins. The Notch extracellular domain (ECD) consists of a series of EGF-like repeats followed by a negative regulatory region (NRR) composed of 3 LIN12/Notch repeats (LNRs) and a heterodimerization domain (HD). The Notch intracellular domain (ICD) contains RAM and ankyrin repeat domains that participate in protein:protein interactions and a C-terminal PEST (proline, glutamate, serine, threonine) degron that regulates protein stability (4).

Notch signaling is stimulated when a Notch receptor interacts with a ligand on a neighboring cell. In mammals there are four canonical activating Notch ligands: two Delta-like ligands (DLL1 and DLL4) and two Jagged ligands (JAG1 and JAG2). Ligand binding leads to cleavage of Notch by a protease of the ADAM family at a site called S2 within the NRR domain. This ligand-dependent cleavage step generates the substrate for subsequent cleavage of the Notch receptor by the γ-secretase complex. Following γ-secretase cleavage, the intracellular domain of Notch (ICD) translocates to the nucleus where it interacts with the DNA-binding factor RBPJ and co-activators of the mastermind-like (MAML) family to form a transcriptional activation complex. Increased expression of target genes, such as members of the HES/HEY family of transcriptional repressors, appears to mediate most Notch functions.

Notch receptors have been implicated as oncogenic drivers in a number of different human cancers. Activating mutations involving two different regions of NOTCH1 are present in >50% of T-cell acute lymphoblastic leukemia (T-ALL) (5). One class of mutations cluster in the hydrophobic core of the HD domain, or occur (albeit infrequently) in the LNR domain (6). These NRR mutations typically act by destabilizing or completely unfolding the HD domain, relaxing the interface that protects the S2 site (7). The second class of mutations consists of frameshifts or stop codons that result in loss of the PEST domain at the C-terminus of the protein. ICD levels are tightly regulated and phosphorylation of the PEST domain and subsequent ubiquitination are postulated to target the ICD for degradation by

E3-ubiquitin ligases such as FBXW7. This negative regulatory axis is abrogated by deletion of the PEST domain, resulting in increased ICD stability and half-life. Similar PEST mutations also occur in NOTCH1 in a minority of chronic lymphocytic leukemias and mantle cell lymphomas, as well as in NOTCH2 in a subset of splenic marginal zone lymphomas (8).

In solid tumors, the roles of various Notch receptors in tumor initiation and progression are more complex (9). Rearrangements of NOTCH1 or NOTCH2 identified recurrently in estrogen receptor (ER) negative breast cancer delete most of the coding sequence for the extracellular domain including the NRR, leading to expression of constitutively active Notch polypeptides (10, 11). Activating NOTCH1 mutations involving the NRR and PEST domains that are structurally similar to those found in T-ALL occur in roughly 10% of adenoid cystic carcinomas (12, 13). NOTCH3 has been reported to be amplified in ~ 10-25% of ovarian adenocarcinomas (14-16). In large-scale cancer genome efforts, NOTCH3 mutations have also been reported in around 1% of head and neck squamous carcinomas, ovarian cancers and lung adenocarcinoma. However, in many studies high GC content has resulted in poor sequencing depth of NOTCH3 exons 25 and 33, where activating mutations are most likely to be found based on prior studies of NOTCH1 and NOTCH2 in hematologic cancers. Thus, although the Notch pathway is an attractive target for novel therapies, the full extent of activation of Notch receptors in human cancer remains to be determined. In addition, NOTCH3 is an attractive target as it displays more restricted tissue expression than other NOTCH receptors and NOTCH3 specific therapies might be predicted to have less toxicity. For instance, gastrointestinal toxicity, observed clinically upon gamma secretase treatment (17), has been attributed to inhibition of NOTCH1 and NOTCH2 based on studies in mouse models (18) In addition, NOTCH1 and NOTCH2 receptor knockout mice are embryonic lethal (19-22) where as NOTCH3 knockout mice are viable and fertile (23), with phenotypes limited to structural defects in arterial vascular smooth muscle cells (24).

Characterization of cellular models and tumors with NOTCH1 activating mutations has been aided by antibody reagents that specifically detect the neo-epitope that is created by gamma-secretase cleavage. To characterize the role of NOTCH3 in human cancers we took a two-step approach that involved comprehensive sequencing of the NRR and PEST domains of NOTCH3 in a panel of cell lines, and generation of an antibody that specifically detects the neo-epitope at the N-terminus of activated NOTCH3 (ICD3) that is created by gamma-secretase cleavage. Here, we describe several mutations in the NRR and PEST domains that result in NOTCH3 activation (“activating mutations”), including an NRR mutation in the human T-ALL cell line, TALL-1 that leads to ligand-independent receptor activation. We also describe two new inhibitory antibodies that suppress ligand-dependent and -independent NOTCH3 signaling by binding to the NOTCH3 NRR and exhibit anti-leukemic activity in cell lines and tumor xenografts. By screening 40 primary T-ALL tumors and 24 orthotopic patient-derived xenograft (PDX) models with an ICD3-specific antibody, we also identified two primary tumors and 12 PDX models with evidence of ongoing NOTCH3 activation. These findings offer a path forward for identification of cancers that are likely to respond to therapy with NOTCH3 selective inhibitory antibodies.

Results

Identification and characterization of the NOTCH3 S1580L NRR mutation

Multiple T-ALL cell lines with activating NOTCH1 mutations have been characterized (5), and several of these cell lines depend on Notch signaling for proliferation and are sensitive to gamma secretase inhibitors (GSIs). Characterization of a panel of T-ALL cell lines to a well-characterized GSI (DAPT), confirmed that the cell line TALL-1 showed a dose dependent decrease in proliferation (Fig. 1A), similar to the T-ALL cell line HPB-ALL, which is GSI-sensitive and has activating NOTCH1 mutations in both the NRR and PEST domains (5). Although TALL-1 has no known alterations in NOTCH1, it harbors a homozygous mutation in exon 26 (c4739t) of NOTCH3. This mutation produces a S1580L point substitution in the NRR domain that leads to increased ligand-independent NOTCH3 activation . TALL-1 also displays an mRNA signature of Notch pathway activity (Supplemental Fig. 1). When a panel of T-ALL cell line lysates was examined with an anti-NOTCH3 antibody, blots of TALL-1 cell lysates showed antibody-reactive bands with molecular weights between 97 and 64kDa (Fig. 1B). TALL-1 cells lacked detectable ICD1, unlike other T-ALL lines with well characterized NOTCH1 activating mutations such as HPB-ALL, RPMI8402, DND41 and Jurkat (Fig. 1B). Moreover, when introduced into a chimeric NOTCH3 construct containing the extracellular and transmembrane domains of NOTCH3 and an intracellular domain consisting of the Gal4 DNA binding domain and the VP16 transactivation domain, the S1580L point substitution mutation results in an approximately 10-fold increase in activation of a Gal4-reporter gene relative to the wild-type NOTCH3-Gal4 fusion control (Fig. 1D), consistent with studies of the basal activity of the S1580L mutation recently reported elsewhere (25). Wild-type and mutated receptors in this assay were present in approximately equal amounts as determined by flow cytometry (Fig. 1D), excluding the possibility that the increased signal in various assays for activity results from increased protein abundance on the cell surface. Prior work has shown that TALL-1 cells, lack activating mutations in NOTCH1 (5) and are resistant to inhibitory antibodies specific for the NRR of NOTCH1 (26). These data confirm that the S1580L mutation activates NOTCH3 signaling independent of ligand stimulation and is responsible for Notch pathway dependence in the TALL-1 cell line.

Development of an ICD3 neo-epitope antibody for monitoring NOTCH3 signaling

To detect the activated form of NOTCH3, we generated a custom antibody specific for the neo-epitope in human NOTCH3 ICD (ICD3) that is created by gamma-secretase cleavage between amino acids G1661 and V1662. To characterize this antibody we screened a panel of T-ALL lines by Western blotting. An antibody-reactive band sensitive to the gamma-secretase inhibitor DAPT was only detected in TALL-1 cells, indicating that the antibody recognizes ICD3 and does not cross-react with ICD1 (Fig. 2A, B). The strong ICD3 signal in TALL-1 cells also provides further evidence that the S1580L mutation leads to an increase in NOTCH3 activation.

Identification and characterization of cell lines with NOTCH3 NRR and PEST mutations

To determine the frequency of NOTCH3 mutations in other cell lines, we analyzed next generation sequencing (NGS) data of 947 cancer cell lines from the Cancer Cell Line

encyclopedia (CCLE) (27). Although NOTCH3 was one of the genes sequenced, examination of the data revealed that sequencing depth of NOTCH3 exons 25 and 33 was insufficient in most cases to permit the identification of mutations (Supplemental Table 1). Therefore, Sanger Sequencing (Genewiz), RainDance analysis (28) and RNAseq (29) were performed to determine whether any of these cell lines had NOTCH3 mutations. Mutations were found in both the NRR and PEST regions (Supplemental Tables 2, 3) in various cell lines, which were further characterized by Western blot analysis with the ICD3 antibody. This revealed high levels of ICD3 in the endometrial cancer cell line Ishikawa, which has an N1597K mutation in the NOTCH3 NRR domain (Fig 2C). Elevated ICD3 was also detected in three cell lines with PEST domain mutations, MDA-MB468 breast carcinoma cells and A549 and NCI-H2347 lung carcinoma cells (Fig. 2D). MDA-MB468 cell extracts contained two forms of ICD3, a prominent truncated form consistent with the presence of a frameshift mutation involving codon 2034 and a second polypeptide of the expected sized of full-length ICD3. The higher levels of the smaller polypeptide with the PEST deletion in MDA-MB468 cells suggests that it has a longer half-life than wild-type ICD3, as previously shown for forms of ICD1 containing PEST deletions (4).

Characterization of Inhibitory anti-NOTCH3 Antibodies in Cell Lines with Mutated or Amplified NOTCH3

To determine if cell lines with NOTCH3 abnormalities depend on NOTCH3 signaling for growth, we used phage display to isolate antibodies against the NRR and ligand binding domains (LBD) of NOTCH3, and then tested these antibodies for their ability to inhibit NOTCH3 signaling (30-32). We focused our studies on three antibodies against the NRR domain and one antibody against the LBD domain. The binding of NOTCH3 antibodies to recombinant proteins and to cells expressing NOTCH3 was analyzed using several complementary methods, including flow cytometry and surface plasmon resonance, which shows very slow off rates for antibody-NRR complexes (Supplemental Figure 2, 3). We examined the effect of each antibody on NOTCH3 signaling in TALL-1 cells by assessing their effects on Notch target gene expression (Fig. 3A). NOTCH3 antibodies against the NRR domain (MOR20350, MOR20358, MOR20337, and the previously characterized anti-NOTCH3 NRR antibody A4 (33) inhibited expression of the Notch target genes DTX1, HES1, NOTCH3 and PTCRα, whereas the anti-LBD antibody (MOR20364) did not. The inhibition achieved with the MOR20350 and MOR20358 anti-NOTCH3 antibodies was comparable to that produced by GSI treatment. In contrast, RPMI-8402, a T-ALL line with activating NOTCH1 mutations and readily detectable ICD1 that lacks ICD3, did not downregulate Notch target genes in response to anti-NOTCH3 NRR antibodies, but did so in response to GSI (Supplemental Fig. 4). Consistent with these findings, ICD3 levels were reduced in TALL-1 cells upon treatment with anti-NRR antibodies, whereas the anti-LBD antibody (MOR12229) had no effect on ICD3 levels. Treatment of the NOTCH3 PEST mutated cell line MDA-MB468 with NOTCH3 NRR antibodies (MOR20337, MOR20350 and MOR20358) decreased ICD3 levels, but treatment with the LBD antibody 20802 did not. In other cells lines with NOTCH3 mutations including A549, TE-11 and Ishikawa (Supplemental Fig. 5) treatment with the anti-NRR antibody MOR20350 substantially decreased ICD3 levels. In HCC1143 cells, which have an amplification of NOTCH3 (34), treatment with each NOTCH3 antibody decreased ICD3 levels (Supplemental Fig. 5), with

MOR20350 having the greatest effect. These data suggest that there are at least two mechansims by which NOTCH3 signaling may be activated in cellular models, amplification/overexpression and NRR/PEST mutation.

We next examined whether cell lines with active NOTCH3 signaling are dependent on signaling for growth. Treatment of TALL-1 cells with MOR20350, MOR20358, MOR20337 antibodies or the A4 antibody (33) significantly inhibited TALL-1 proliferation in a dose-dependent manner (Fig. 3C), whereas treatment with NOTCH3 LBD antibodies did not. When NOTCH3 antibodies were tested against a panel of other T-ALL cell lines that are NOTCH1 and NOTCH3 wild-type (SUPT11) or NOTCH1 mutated (HPB-ALL, DND41, P12-Ichikawa, SUPT1, and RPMI-8402), no effects on proliferation were seen (Supplemental Fig. 4 and data not shown). Treatment of MDA-MB468 cells with anti-NOTCH3 NRR antibodies produced a trend toward growth inhibition, but the results were not statistically significant (not shown).

NOTCH3 NRR antibodies bind to distinct non-overlapping epitopes

In an effort to further understand how MOR20350 and MOR20358 inhibit NOTCH3 signaling, we determined the structures of Fab-NOTCH3 NRR complexes using X-ray crystallography. Statistics for X-ray crystallography are summarized in Supplemental Table 6. The NOTCH3 NRR (described in detail in reference (25)) fold is similar to that of NOTCH1 NRR (6, 35, 36) and NOTCH2 NRR (37). The structure of the NOTCH3 NRR/MOR20350 Fab complex (Fig. 4A) was used to identify the binding epitope, which consists of several discontinuous (*i.e.* noncontiguous) sequences from the NRR (Supplemental Table 4 and Supplemental Fig. 6) Notably, the β4-α3 loop in the NOTCH3 HD domain is structurally unique from that of NOTCH1 and NOTCH2, and a majority of this segment is part of the MOR20350 epitope. Furthermore, this loop is mostly unstructured (no electron density due to flexibility) in the NOTCH3/MOR20358 NRR complex, but is structured in the MOR20350 complex due to direct binding to the Fab. The MOR20350 Fab also contacts the LNR region (mainly around LNR-B) of the NOTCH3 NRR (Fig. 4C). These contacts suggest that binding of MOR20350 clamps the LNR and HD domains together, stabilizing the autoinhibitory conformation of the NOTCH3 NRR and blocking NOTCH3 activation.

As with the NOTCH3 NRR/MOR20350 complex, the interaction surface on the NOTCH3 NRR of the MOR20358 Fab is also discontinuous (Fig. 4A, Supplemental Table 5, Supplemental Fig. 6). The structure of the LNR-B/C linker plus the first half of LNR-C of NOTCH3 is unique from those of NOTCH1 and NOTCH2, and most of this segment contacts MOR20358. The MOR20358 Fab also simultaneously binds LNR-C and the HD domain (mainly around the α3-β5 loop), suggesting that it also stabilizes the autoinhibitory conformation of the NOTCH3 NRR.

To determine whether the epitopes of MOR20350 and MOR20358 overlap, the crystal structures of the NOTCH3 NRR/MOR20350 and NOTCH3 NRR/MOR20358 complexes were superimposed on the structure of the NOTCH3 NRR (Fig. 4B). The superposition clearly shows that MOR20350 and MOR20358 bind distinct non-overlapping epitopes within the NOTCH3 NRR. The binding site for the anti-NOTCH3 A4 antibody (33)

constitutes a third epitope (Supplemental Fig. 6), indicating that there are at least three distinct binding modes by which anti-NRR antibodies can allosterically inhibit NOTCH3.

NOTCH3 antibodies display *in vivo* activity against TALL-1 cells

Having established that NOTCH3 antibodies inhibit signaling in cell lines with NOTCH3 mutations *in vitro*, we asked whether these antibodies also have anti-tumor effects *in vivo* using representative cell lines with a NOTCH3 PEST (MDA-MB468) or NRR (TALL-1) mutation, respectively. Tumors from mice engrafted with TALL-1 (Fig. 5A) or MDA-MB468 (Supplemental Fig. 8) cells were treated with NOTCH3 antibodies and evaluated for effects on the expression of Notch target genes and ICD3 levels. Treatment of TALL-1 xenografts with NRR antibodies, but not with LBD antibodies, sharply decreased the expression levels of DTX1 relative to levels in xenografts from animals treated with an IgG control antibody (MOR3207) (Fig. 5A). In addition, treatment with NRR antibodies substantially lowered ICD3 levels relative to control IgG (Fig. 5B). Interestingly, the level of total NOTCH3 was also decreased in TALL-1 tumors treated with NRR antibodies, consistent with autoregulation of NOTCH3 expression by ICD3 itself. Staining of xenografts with ICD3 specific antibody revealed that although there was decreased ICD3 staining following NOTCH3 antibody treatment, some cells within the tumor showed persistent ICD3 expression (Fig. 5B and Supplemental Fig. 8). ICD3 staining was weaker and more heterogeneous in the MDA-MB468 tumors than the TALL-1 tumors (Compare Fig. 5B and Supplemental Fig. 8). These studies showed that NOTCH3 NRR antibodies are capable of inhibiting NOTCH3 signaling *in vivo*.

To further evaluate the anti-tumor effects of NOTCH3 antibodies in the TALL-1 xenograft model, the cell line was luciferized in order to monitor xenograft growth *in vivo*. The MOR20358 and MOR20350 antibodies showed the most anti-tumor activity in this study as compared to animals treated with the control antibody MOR3207 (Fig. 5C). By day 43, no luminescent cells were detected in the cohort treated with MOR20350 (Fig. 5C). Despite inhibition of NOTCH3 signaling by NRR antibodies in the MDA-MB468 xenograft model there was no effect on tumor growth (Supplemental Fig. 8). Therefore, only a subset of cell line models with NOTCH3 mutations retain dependence on NOTCH3 signaling for growth *in vivo*. In an effort to understand the epidemiology of activated NOTCH3 signaling in primary T-ALL samples, 40 patient samples were stained with the ICD3 antibody. Two tumors were identified with high homogenous levels of ICD3 staining, consistent with activation of signaling (Fig. 6A). In an effort to determine if NOTCH3 is mutated in these specimens, we isolated DNA from them but were unable to obtain high quality NOTCH3 sequencing data, likely due to the inherent difficulties of sequencing this gene and the confounding effects of treatment of bone marrow biopsies with highly acidic decalcification solutions as part of their processing. Because of the difficulties of working with archival marrow samples, we further explored the extent of NOTCH3 activation in cell pellets prepared from 24 orthotopic T-ALL PDX models. Remarkably, Western blotting for ICD3 and ICD1 demonstrated activation of NOTCH3 in 12 of 24 models, two of which had activation only of NOTCH3 (Figure 6B), suggesting that activation of NOTCH3 signaling in T-ALL is more prevalent than thought previously. There was a correlation between high

levels of total NOTCH3 and presence of ICD3 which was not observed when we compare levels of total NOTCH1 and presence of ICD1.

Discussion

Studies to examine alternations in Notch signaling in human cancer have identified a spectrum of mutations as well as other genetic alterations including chromosomal translocations in a diverse set of tumor types. However, despite these advances many of these alternations have not been fully characterized. In this study we determined the extent of NOTCH3 NRR and PEST mutations in a panel of cancer cell lines and analyzed for the presence of activated NOTCH3 signaling. Through structural studies NOTCH3 inhibitory antibodies were shown to bind to conformation epitopes on the NRR and lock this domain in the autoinhibited form. The antibodies block NOTCH3 signaling in cell lines and in tumor xenografts, and the TALL-1 cell line dramatically inhibit cellular proliferation and tumor growth.

Activating mutations in the NRR and PEST domains of NOTCH1 have been extensively characterized in T-ALL and shown to be oncogenic drivers in this leukemia (38). Previous mouse models relying on overexpression of ICD3 demonstrated that activation of NOTCH3 signaling can drive T-ALL development (39). Here, we examined a proof of concept mutation in the NOTCH3 NRR domain (S1580L) in a T-ALL cell line, TALL-1, that lacks NOTCH1 activating mutations. The S1580L mutation leads to ligand-independent increases in NOTCH3 signaling and drives a Notch-dependent gene signature that is similar to that seen in T-ALL lines with NOTCH1 mutations (Supplemental Fig. 1 and Fig. 1D). In the NOTCH3 NRR, the side-chain oxygen of S1580 (in HD-C) forms a hydrogen bond with the backbone nitrogen of P1521 (in HD-N). S1580L mutation eliminates this hydrogen bond and likely weakens the interaction between HD-N and HD-C (25). Considering the close proximity of S1580 to the S2 site (~10 Å), this substitution likely makes the S2 site more accessible to ADAM metalloproteases. TALL-1 cells indeed contain markedly elevated levels of ICD3 (Fig. 2 and 5) and are dependent on NOTCH3 signaling for growth and survival *in vitro* and *in vivo*. This dependence is strikingly revealed by the *in vivo* studies, as treatment of mice with the inhibitory antibody MOR20350 resulted in no detectable TALL-1 luminescent cells at the end of the study (Fig. 5C).

Among the NOTCH3 inhibitory antibodies tested, MOR20350 most consistently inhibited NOTCH3 signaling in the broadest spectrum of models with NOTCH3 point substitutions or amplifications. This is likely not explained by differences in antibody binding, as the three NRR antibodies have similar affinities to recombinant NOTCH3 protein and show similar binding to surface NOTCH3 in flow cytometric studies (Table 1). MOR20350, as compared to MOR20358, has a larger binding interface on the surface of the NOTCH3 NRR and this interface is more evenly distributed between the LNRs and the HD (Fig. 4C). In addition, the binding interface lies close to LNR-A, which harbors a conserved leucine residue (L1419) that is responsible for packing of the α3 helix against the S2 site on β5, thereby precluding access of ADAM metalloproteases. The likely mode of action of our antibodies is consistent with other studies showing that inhibitory Notch antibodies binding the NRR domain and recognize epitopes that span the LNR and HD domains (36) *via* the NOTCH3 NRR (A4)

(33). Comparison of the structures of MOR20350 and MOR20358, antibodies bound to the NOTCH3 NRR domain as well as previously published binding epitope information for A4 (33, 40) show that each binds a distinct epitope, (Fig. 4B and Supplemental Fig. 6). Therefore, there are multiple regions on the surface of the NRR where antibodies can bind and stabilize LNR-HD interaction.

Identification of Notch signaling alterations in human tumors has emerged from cancer genome sequencing data as well as development of reagents to detect Notch pathway activation. Recently, NOTCH1, NOTCH2 and NOTCH3 mutations were identified in an analysis of the breast cancer TCGA dataset, with enrichment of mutations in the triple negative sub-type (41). The authors noted five tumors with NOTCH3 PEST domain mutations but were unable to characterize NOTCH3 signaling activation due to lack of samples or primary tumor xenograft models. In an examination of NOTCH3 mutations from cancer genome sequencing studies, we also identified multiple diverse tumors with NRR or PEST mutations (Supplemental Table 7) A reliable antibody reagent to detect the active NOTCH1 ICD1 has been identified and protocols developed for IHC stains that enable screening of archival tumor samples for NOTCH1 activation (42). In this study we report the development of a similar reagent to detect the active form of NOTCH3, ICD3. This reagent was used to screen 40 T-ALL bone marrow samples, two of which had detectable ICD3 staining, but attempts to sequence tumor DNA samples from de-calcified and fixed bone marrow samples, which are known to pose challenges, were unsuccessful. However, 12/24 orthotopic T-ALL PDX samples showed readily detectable NOTCH3 activation, two of which showed activation only of NOTCH3. DNA sequencing of these models did not reveal any NOTCH3 mutations,suggesting that NOTCH3 activation either is mutation- and ligand-independent or mutation-independent and ligand dependent. The former possibility is in line with our data that total NOTCH3 protein is high in models with detectable ICD3 and with studies showing that among mammalian Notch receptors, NOTCH3 has the highest propensity for spontaneous activation, possibly because it's NRR is less tightly locked in the ADAM metalloprotease resistant state (25). In addition, models with NOTCH3 amplification/overexpression such as HCC1143 also show evidence of activated NOTCH3 signaling (Supplemental Fig. 5). Alternatively, NOTCH3 activation could be ligand dependent in these models, which is consistent with expression of the Notch ligands such as JAG1 and DLL4 in the bone microenvironment (43, 44). A complete understanding of the extent to which NOTCH3 signaling activation populates the T-ALL landscape as well as other cancers will require screening of a large collection of samples and follow-up detailed mechanistic studies. Pre-screening of these samples with the ICD3 antibody should identify the subset of tumor samples with the highest likelihood of harboring NOTCH3 mutations. Ultimately a combination of genome sequencing as well as reagents that can detect NOTCH3 activation will enable identification of patients who may be effectively treated with NOTCH3 antibodies, such as those reported here.

Materials and Methods

Cell Lines and PDX Models

Cell lines and PDX models were routinely authenticated by SNP fingerprinting and tested for mycoplasma. HPB-ALL was obtained from Andreas Strasser. TALL-1, RPMI-8402, SUPT11, Loucy, P12-Ichikawa, PF382 were purchased from DSMZ. Jurkat (clone E6-1), U2OS, MDA-MB-468, HCC1143 were purchased from ATCC. HLR PathDetect cells were purchased from Stratagene. All other cell lines were obtained from the Novartis stocks of the Cancer cell line encyclopedia (27). T-ALL PDX models were created from primary T-ALLs by injection by tail vein into immunodeficient NOD/Scid/IL2rγ^{null} (NSG) mice and are described at the online portal PRoXe at http://PRoXe.org. Detergent extracts of T-ALL cells obtained from the marrows of leukemia-bearing mice were analyzed for activated NOTCH1 (ICD1) and activated NOTCH3 (ICD3) by Western blotting.

Notch Target Gene mRNA Assay

To quantitate DTX1 and NOTCH3 mRNA levels, 1×10^4 TALL-1 cells/well were plated and the antibody and compound dilutions were added to each well. DAPT (Calbiochem, cat#565770) and DMSO were used for this assay. Cells were incubated with antibody or compound for 72hr. TaqMan gene expression assays were run with gene expression probes for DTX1 (Hs00269995_m1, Life Technologies) or NOTCH3 (Hs01128541_m1, Applied Biosystems) and the housekeeping gene PP1A (Hs99999904_m1, Life Technologies). To quantitate the levels of each target gene, 2–[delta][delta]Ct method was employed (45).

TALL-1 Cell Proliferation Assays

1×10^4 TALL-1 cells/well were seeded into 96-well tissue culture plates, in the presence of anti-NOTCH3 antibody for varying times. Cell numbers were determined by quantifying ATP levels with, CellTiter-Glo reagent (Promega).

In vivo studies

All *in vivo* studies conducted were performed in strict accordance with the Novartis animal welfare policies. No blinding was used for the animal studies. For TALL-1 xenograft studies, female SCID-beige mice were inoculated with 10×10^6 cells. Once tumors reached between 300 and 500 mm^3 (n=3/group), mice were randomly assigned to receive a single intravenous 20 mg/kg dose of MOR3207 (IgG control), MOR20350, MOR20358 or MOR20802 and ICD3 was evaluated by Western blot. To generate a TALL-1 cell line with constitutive expression of luciferase, the TALL-1 cell line was transduced with pMMP-LucNeo. To assess *in vivo* activity of NOTCH3 antibodies mice were inoculated with 10×10^6 T-ALL1_Luc cells. Tumor growth was monitored using the Xenogen *in vivo* imaging system (Caliper Life Sciences). On day 11, tumor-bearing animals were randomly assigned to receive intravenous doses of either PBS or 20 mg/kg of negative control IgG antibody (n=8/group) or the NOTCH3 antibodies twice per week.

X-ray crystallography

The NOTCH3 NRR was expressed as a secreted protein in HEK293S GnTI- cells (ATCC). For additional details please see Supplemental Materials and Methods. The structures of the Notch3-antibody complexes have been submitted to the Protein Data Bank (PDB) (46) and can be found under accession number 5CZV (20350 complex) and 5CZX (20358 complex).

Supplementary Material

Refer to Web version on PubMed Central for supplementary material.

Acknowledgments

The JAGGED1 and DLL1 expressing cell lines were kindly provide by Dr. Gerry Weinmaster (UCLA). HPB-ALL cells were kindly provided by Andreas Stasser (Walter and Eliza Hall Institute for Medical Research, Australia). The authors thank the Novartis Biologics Center including Thomas Pietzonka, Janine Shulok, Nadine Charara, Bill Tschantz and Tony Fleming. We also thank many senior Novartis leaders for supporting this project, including Jeff Porter and William Sellers. We thank Rajiv Chopra and Kirk Clark of Novartis Institutes for BioMedical Research for the instructive discussion on crystallography experiments. Use of the IMCA-CAT beamline 17-ID at the Advanced Photon Source was supported by the companies of the Industrial Macromolecular Crystallography Association through a contract with Hauptman–Woodward Medical Research Institute. Use of the Advanced Photon Source was supported by the U.S. Department of Energy, Office of Science, Office of Basic Energy Sciences, under Contract No. DE-AC02-06CH11357. This work was financially supported in part by the Dana Farther-Novartis DDP, and grants from the National Institutes of Health (P01 CA119070) and the Leukemia and Lymphoma Society (7003-13).

References

1. Kopan R, Ilagan MX. The canonical Notch signaling pathway: unfolding the activation mechanism. Cell. 2009; 137(2):216–33. [PubMed: 19379690]
2. Guruharsha KG, Kankel MW, Artavanis-Tsakonas S. The Notch signalling system: recent insights into the complexity of a conserved pathway. Nature reviews Genetics. 2012; 13(9):654–66.
3. Andersson ER, Sandberg R, Lendahl U. Notch signaling: simplicity in design, versatility in function. Development. 2011; 138(17):3593–612. [PubMed: 21828089]
4. Fryer CJ, White JB, Jones KA. Mastermind recruits CycC:CDK8 to phosphorylate the Notch ICD and coordinate activation with turnover. Molecular cell. 2004; 16(4):509–20. [PubMed: 15546612]
5. Weng AP, Ferrando AA, Lee W, Morris JPt, Silverman LB, Sanchez-Irizarry C, et al. Activating mutations of NOTCH1 in human T cell acute lymphoblastic leukemia. Science. 2004; 306(5694): 269–71. [PubMed: 15472075]
6. Gordon WR, Roy M, Vardar-Ulu D, Garfinkel M, Mansour MR, Aster JC, et al. Structure of the Notch1-negative regulatory region: implications for normal activation and pathogenic signaling in T-ALL. Blood. 2009; 113(18):4381–90. [PubMed: 19075186]
7. Malecki MJ, Sanchez-Irizarry C, Mitchell JL, Histen G, Xu ML, Aster JC, et al. Leukemia-associated mutations within the NOTCH1 heterodimerization domain fall into at least two distinct mechanistic classes. Molecular and cellular biology. 2006; 26(12):4642–51. [PubMed: 16738328]
8. Ntziachristos P, Lim JS, Sage J, Aifantis I. From fly wings to targeted cancer therapies: a centennial for notch signaling. Cancer cell. 2014; 25(3):318–34. [PubMed: 24651013]
9. Ranganathan P, Weaver KL, Capobianco AJ. Notch signalling in solid tumours: a little bit of everything but not all the time. Nature reviews Cancer. 2011; 11(5):338–51. [PubMed: 21508972]
10. Robinson DR, Kalyana-Sundaram S, Wu YM, Shankar S, Cao X, Ateeq B, et al. Functionally recurrent rearrangements of the MAST kinase and Notch gene families in breast cancer. Nature medicine. 2011; 17(12):1646–51.
11. Stoeck A, Lejnine S, Truong A, Pan L, Wang H, Zang C, et al. Discovery of biomarkers predictive of GSI response in triple-negative breast cancer and adenoid cystic carcinoma. Cancer discovery. 2014; 4(10):1154–67. [PubMed: 25104330]

12. Stephens PJ, Davies HR, Mitani Y, Van Loo P, Shlien A, Tarpey PS, et al. Whole exome sequencing of adenoid cystic carcinoma. The Journal of clinical investigation. 2013; 123(7):2965–8. [PubMed: 23778141]
13. Ho AS, Kannan K, Roy DM, Morris LG, Ganly I, Katabi N, et al. The mutational landscape of adenoid cystic carcinoma. Nature genetics. 2013; 45(7):791–8. [PubMed: 23685749]
14. Nakayama K, Nakayama N, Jinawath N, Salani R, Kurman RJ, Shih Ie M, et al. Amplicon profiles in ovarian serous carcinomas. International journal of cancer Journal international du cancer. 2007; 120(12):2613–7. [PubMed: 17351921]
15. Etemadmoghadam D, deFazio A, Beroukhim R, Mermel C, George J, Getz G, et al. Integrated genome-wide DNA copy number and expression analysis identifies distinct mechanisms of primary chemoresistance in ovarian carcinomas. Clinical cancer research : an official journal of the American Association for Cancer Research. 2009; 15(4):1417–27. [PubMed: 19193619]
16. Cancer Genome Atlas Research N. Integrated genomic analyses of ovarian carcinoma. Nature. 2011; 474(7353):609–15. [PubMed: 21720365]
17. Aster JC, Blacklow SC. Targeting the Notch pathway: twists and turns on the road to rational therapeutics. Journal of clinical oncology : official journal of the American Society of Clinical Oncology. 2012; 30(19):2418–20. [PubMed: 22585704]
18. Vooijs M, Liu Z, Kopan R. Notch: architect, landscaper, and guardian of the intestine. Gastroenterology. 2011; 141(2):448–59. [PubMed: 21689653]
19. Krebs LT, Xue Y, Norton CR, Shutter JR, Maguire M, Sundberg JP, et al. Notch signaling is essential for vascular morphogenesis in mice. Genes & development. 2000; 14(11):1343–52. [PubMed: 10837027]
20. Huppert SS, Le A, Schroeter EH, Mumm JS, Saxena MT, Milner LA, et al. Embryonic lethality in mice homozygous for a processing-deficient allele of Notch1. Nature. 2000; 405(6789):966–70. [PubMed: 10879540]
21. Limbourg FP, Takeshita K, Radtke F, Bronson RT, Chin MT, Liao JK. Essential role of endothelial Notch1 in angiogenesis. Circulation. 2005; 111(14):1826–32. [PubMed: 15809373]
22. McCright B, Gao X, Shen L, Lozier J, Lan Y, Maguire M, et al. Defects in development of the kidney, heart and eye vasculature in mice homozygous for a hypomorphic Notch2 mutation. Development. 2001; 128(4):491–502. [PubMed: 11171333]
23. Krebs LT, Xue Y, Norton CR, Sundberg JP, Beatus P, Lendahl U, et al. Characterization of Notch3-deficient mice: normal embryonic development and absence of genetic interactions with a Notch1 mutation. Genesis. 2003; 37(3):139–43. [PubMed: 14595837]
24. Domenga V, Fardoux P, Lacombe P, Monet M, Maciazek J, Krebs LT, et al. Notch3 is required for arterial identity and maturation of vascular smooth muscle cells. Genes & development. 2004; 18(22):2730–5. [PubMed: 15545631]
25. Xu X, Choi SH, Hu T, Tiyanont K, Habets R, Groot AJ, et al. Insights into Autoregulation of Notch3 from Structural and Functional Studies of Its Negative Regulatory Region. Structure. 2015; 23(7):1227–35. [PubMed: 26051713]
26. Aste-Amezaga M, Zhang N, Lineberger JE, Arnold BA, Toner TJ, Gu M, et al. Characterization of Notch1 antibodies that inhibit signaling of both normal and mutated Notch1 receptors. PloS one. 2010; 5(2):e9094. [PubMed: 20161710]
27. Barretina J, Caponigro G, Stransky N, Venkatesan K, Margolin AA, Kim S, et al. The Cancer Cell Line Encyclopedia enables predictive modelling of anticancer drug sensitivity. Nature. 2012; 483(7391):603–7. [PubMed: 22460905]
28. Tewhey R, Warner JB, Nakano M, Libby B, Medkova M, David PH, et al. Microdroplet-based PCR enrichment for large-scale targeted sequencing. Nature biotechnology. 2009; 27(11):1025–31.
29. Wang Z, Gerstein M, Snyder M. RNA-Seq: a revolutionary tool for transcriptomics. Nature reviews Genetics. 2009; 10(1):57–63.
30. Prassler J, Steidl S, Urlinger S. In vitro affinity maturation of HuCAL antibodies: complementarity determining region exchange and RapMAT technology. Immunotherapy. 2009; 1(4):571–83. [PubMed: 20635988]

31. Prassler J, Thiel S, Pracht C, Polzer A, Peters S, Bauer M, et al. HuCAL PLATINUM, a synthetic Fab library optimized for sequence diversity and superior performance in mammalian expression systems. Journal of molecular biology. 2011; 413(1):261–78. [PubMed: 21856311]
32. Rauchenberger R, Borges E, Thomassen-Wolf E, Rom E, Adar R, Yaniv Y, et al. Human combinatorial Fab library yielding specific and functional antibodies against the human fibroblast growth factor receptor 3. The Journal of biological chemistry. 2003; 278(40):38194–205. [PubMed: 12842902]
33. Li K, Li Y, Wu W, Gordon WR, Chang DW, Lu M, et al. Modulation of Notch signaling by antibodies specific for the extracellular negative regulatory region of NOTCH3. The Journal of biological chemistry. 2008; 283(12):8046–54. [PubMed: 18182388]
34. Yamaguchi N, Oyama T, Ito E, Satoh H, Azuma S, Hayashi M, et al. NOTCH3 signaling pathway plays crucial roles in the proliferation of ErbB2-negative human breast cancer cells. Cancer research. 2008; 68(6):1881–8. [PubMed: 18339869]
35. Gordon WR, Vardar-Ulu D, L'Heureux S, Ashworth T, Malecki MJ, Sanchez-Irizarry C, et al. Effects of S1 cleavage on the structure, surface export, and signaling activity of human Notch1 and Notch2. PloS one. 2009; 4(8):e6613. [PubMed: 19701457]
36. Wu Y, Cain-Hom C, Choy L, Hagenbeek TJ, de Leon GP, Chen Y, et al. Therapeutic antibody targeting of individual Notch receptors. Nature. 2010; 464(7291):1052–7. [PubMed: 20393564]
37. Gordon WR, Vardar-Ulu D, Histen G, Sanchez-Irizarry C, Aster JC, Blacklow SC. Structural basis for autoinhibition of Notch. Nature structural & molecular biology. 2007; 14(4):295–300.
38. Chiang MY, Xu L, Shestova O, Histen G, L'Heureux S, Romany C, et al. Leukemia-associated NOTCH1 alleles are weak tumor initiators but accelerate K-ras-initiated leukemia. The Journal of clinical investigation. 2008; 118(9):3181–94. [PubMed: 18677410]
39. Bellavia D, Campese AF, Alesse E, Vacca A, Felli MP, Balestri A, et al. Constitutive activation of NF-kappaB and T-cell leukemia/lymphoma in Notch3 transgenic mice. The EMBO journal. 2000; 19(13):3337–48. [PubMed: 10880446]
40. Tiyanont K, Wales TE, Siebel CW, Engen JR, Blacklow SC. Insights into Notch3 activation and inhibition mediated by antibodies directed against its negative regulatory region. Journal of molecular biology. 2013; 425(17):3192–204. [PubMed: 23747483]
41. Wang K, Zhang Q, Li D, Ching K, Zhang C, Zheng X, et al. PEST domain mutations in Notch receptors comprise an oncogenic driver segment in triple-negative breast cancer sensitive to a gamma-secretase inhibitor. Clinical cancer research : an official journal of the American Association for Cancer Research. 2015; 21(6):1487–96. [PubMed: 25564152]
42. Kluk MJ, Ashworth T, Wang H, Knoechel B, Mason EF, Morgan EA, et al. Gauging NOTCH1 Activation in Cancer Using Immunohistochemistry. PloS one. 2013; 8(6):e67306. [PubMed: 23825651]
43. Calvi LM, Adams GB, Weibrecht KW, Weber JM, Olson DP, Knight MC, et al. Osteoblastic cells regulate the haematopoietic stem cell niche. Nature. 2003; 425(6960):841–6. [PubMed: 14574413]
44. Ramasamy SK, Kusumbe AP, Wang L, Adams RH. Endothelial Notch activity promotes angiogenesis and osteogenesis in bone. Nature. 2014; 507(7492):376–80. [PubMed: 24647000]
45. Livak KJ, Schmittgen TD. Analysis of relative gene expression data using real-time quantitative PCR and the 2(-Delta Delta C(T)) Method. Methods. 2001; 25(4):402–8. [PubMed: 11846609]
46. Berman H, Henrick K, Nakamura H. Announcing the worldwide Protein Data Bank. Nature structural biology. 2003; 10(12):980. [PubMed: 14634627]

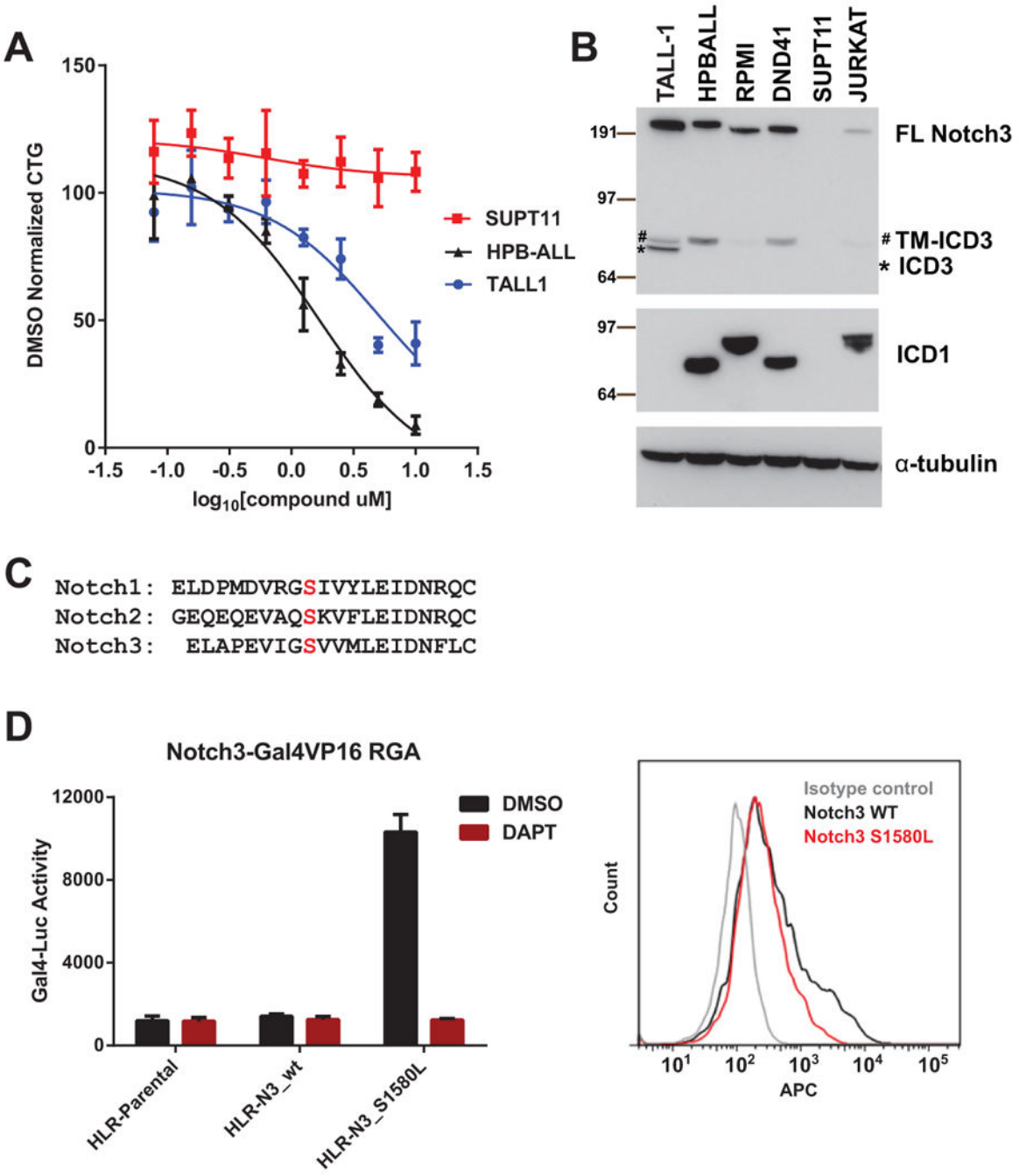

Figure 1. Identification of an activating NOTCH3 NRR mutation in TALL-1 cells

(A) T-ALL cell lines HPB-ALL (NOTCH1 NRR mutant) SUPT11 (NOTCH1 wild-type) and TALL-1 (NOTCH 1 wild-type) were treated with a GSI for 6-7 days and proliferation monitored by Cell Titer-Glo assay. (B) Protein lysates were generated from untreated T-ALL cell lines and lysates probed with antibodies for NOTCH 3, ICD1 and α-tubulin. # TM-ICD3 is the transmembrane-domain-ICD3 subunit produced by furin cleavage of NOTCH3, while * ICD3 is the intracellular domain of Notch3 produced by successive metalloprotease and gamma secretase cleavage. (C) Alignment of a portion of the NOTCH 1, NOTCH 2 and

NOTCH 3 NRR domains. The S1580 residue of NOTCH3 and corresponding serine residues in NOTCH1 and NOTCH2 are highlighted in red. (D) HeLa cell lines with stable expression of GAL4-Luciferase reporter were generated expressing either wild-type or mutant (S1580L) NOTCH 3-GAL4-VP16. Cells were treated with either DMSO or 10μM DAPT for 24hr prior to measuring GAL4-Luciferase activity. The level of NOTCH 3 receptors on the cell surface was determined by binding of anti-NOTCH3 APC labeled antibody to cells expressing mutant and endogenous NOTCH3 and assessed by flow cytometry.

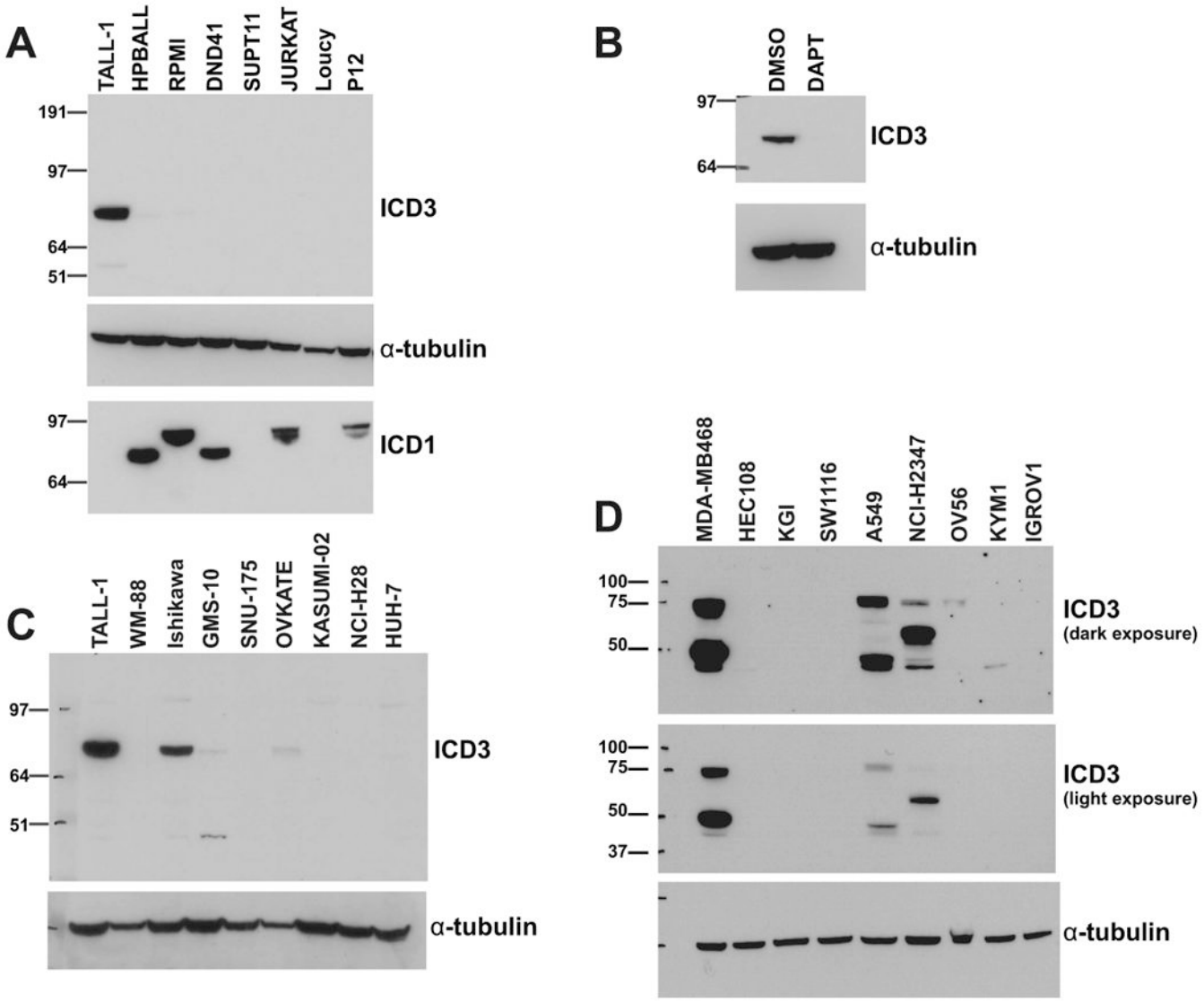

Figure 2. ICD3 antibody detects activated NOTCH 3 in TALL-1 cells and other lines with NOTCH3 NRR and PEST mutations

(A) Protein lysates were generated from untreated T-ALL cell lines and lysates probed with antibodies for ICD3, ICD1 and α-tubulin. (B) TALL-1 cells were treated with the DMSO or 10μM DAPT for 72hr prior to generation of protein lysates for Western blotting with ICD3 antibody and α-tubulin. (C) Protein lysates were generated from untreated cell lines with NRR mutations and lysates probed with antibodies for ICD3 and α-tubulin. (D) Protein lysates were generated from untreated cell lines with PEST mutations and lysates probed with antibodies for ICD3 and α-tubulin.

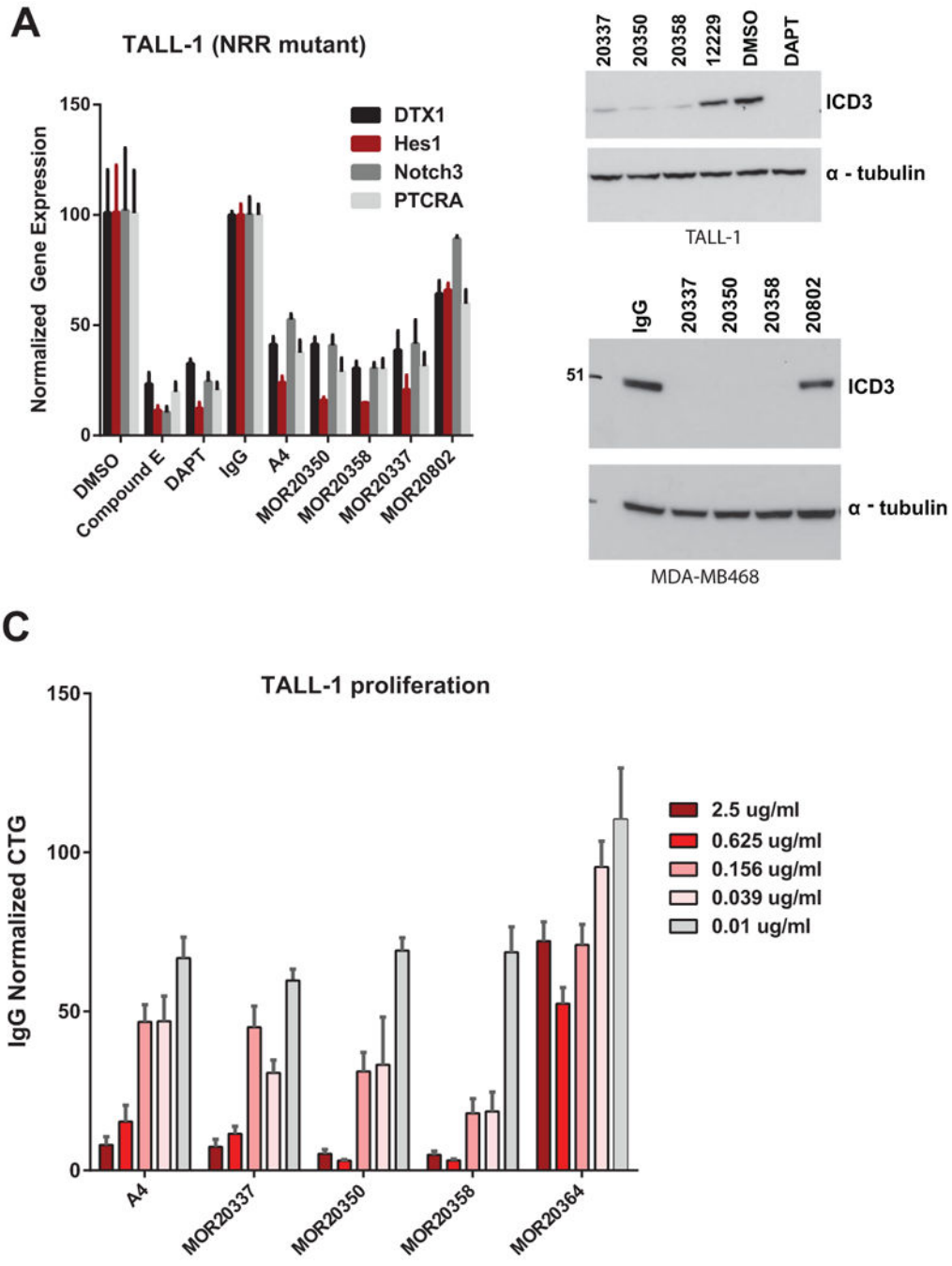

Figure 3. Identification and characterization of NOTCH3 inhibitory antibodies

(A) TALL-1 cells were treated with 10μg/ml IgG control antibody or NOTCH3 NRR antibodies (A4, MOR20337, MOR20350, and MOR20358) or NOTCH3 LBD antibody (MOR20364) for 72hrs prior to quantitation of DTX1 mRNA levels by qRT-PCR. Positive and negative control TALL-1 cells were treated with DMSO or 10μM DAPT for 72hrs. (B) Effect of treatment of TALL-1 cells and MDA-MB468 cells with NOTCH3 NRR antibodies on levels of ICD3. (C) Effect of treatment of TALL-1 cells with NOTCH3 NRR antibodies on proliferation.

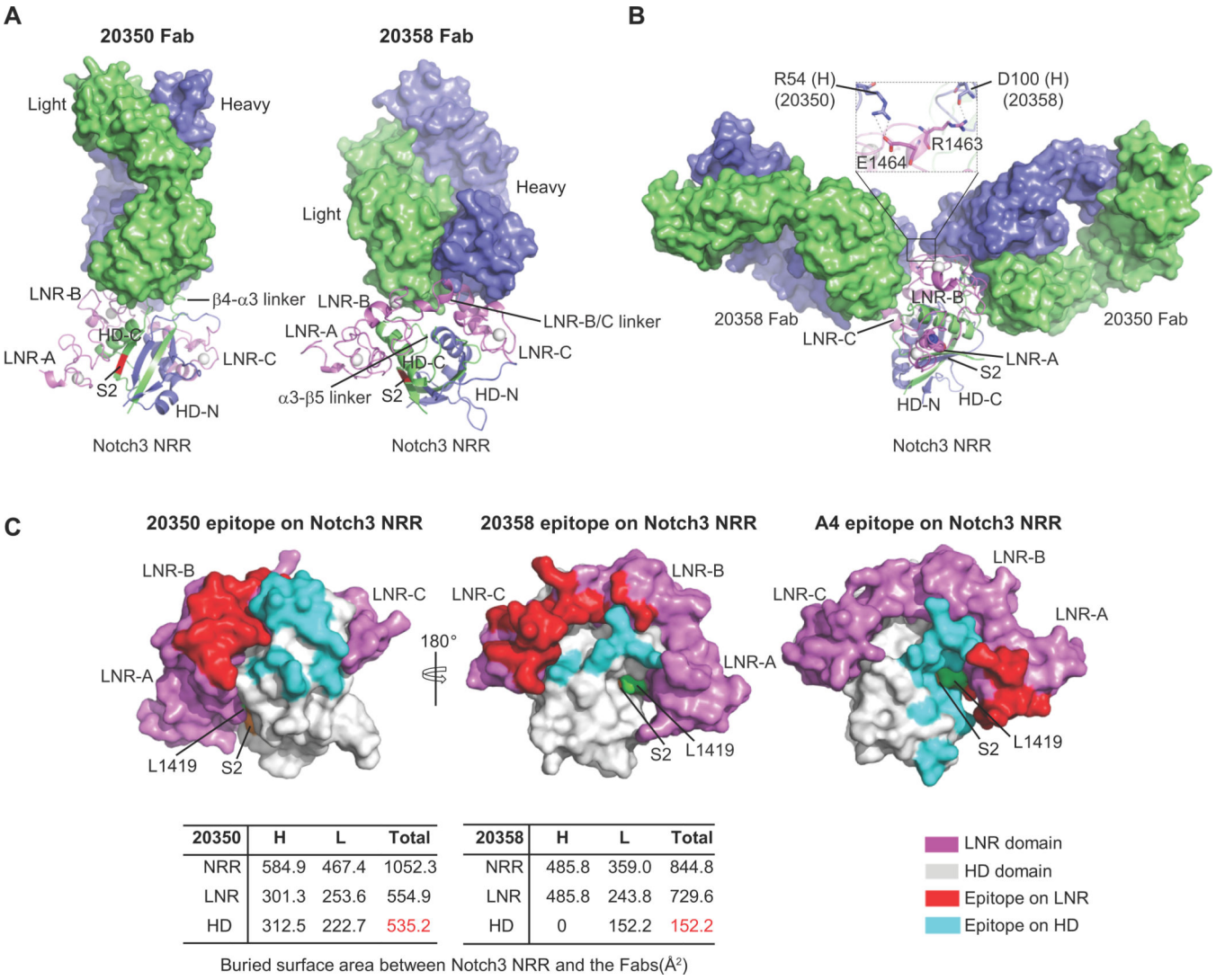

20350	H	L	Total
NRR	584.9	467.4	1052.3
LNR	301.3	253.6	554.9
HD	312.5	222.7	535.2

20358	H	L	Total
NRR	485.8	359.0	844.8
LNR	485.8	243.8	729.6
HD	0	152.2	152.2

Figure 4. Crystallographic determination of epitopes by MOR20350 and MOR20358

(A) Overall structures of MOR20350 and MOR20358 binding to NOTCH3 NRR. (B) Structural superposition of MOR20350 and MOR20358 complexes on NOTCH3 NRR, showing non-overlapping epitopes of the two antibodies. (C) Epitopes of MOR20350, MOR20358 and A4 (red and cyan) are shown on the surface of NOTCH3 NRR. The buried surface areas of MOR20350 and MOR20358 binding to NOTCH3 NRR are also listed.

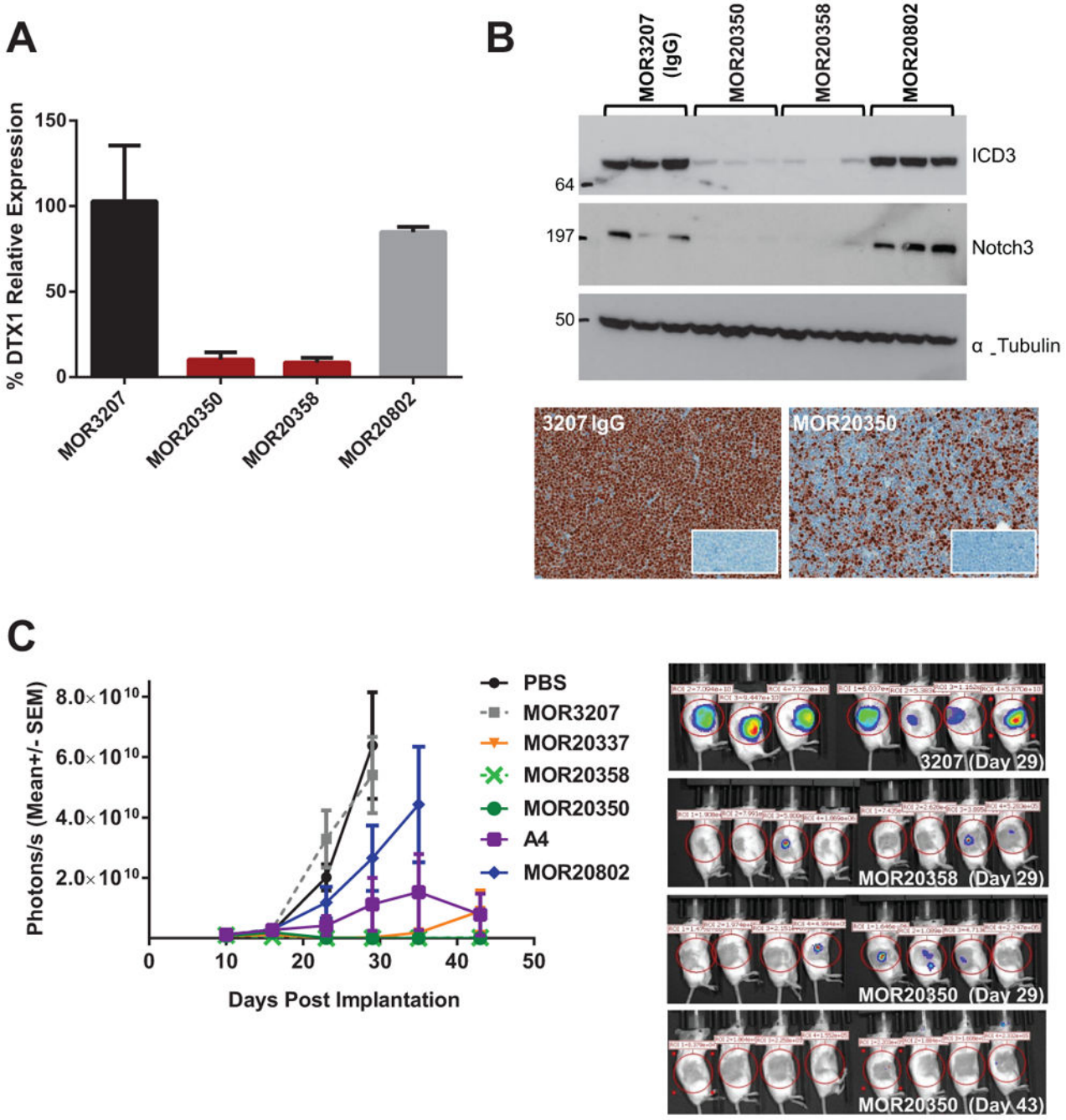

Figure 5. NOTCH3 NRR antibodies inhibit NOTCH3 signaling *in vivo* and are efficacious in a TALL-1 xenograft model

Mice bearing luciferized TALL-1 xenografts were dosed intravenously with a single 20mg/kg dose of the indicated antibody. Tumors were harvested 72hr later and analyzed for (A) expression of DTX1 mRNA by qRT-PCR (NRR antibodies are shown in red while LBD antibodies are shown in grey) or (B) ICD3 and total NOTCH3 by Western blot. In addition, a portion of tumor was fixed in formalin and analyzed by immunohistochemical staining with the ICD3 antibody or an isotype control IgG (inset). (C) Mice bearing luciferized TALL-1 xenografts were dosed intravenously with the indicated antibodies at 20mg/kg twice per

week starting on day 11 after implantation of tumor cells. Tumor size was monitored with the Xenogen in vivo imaging system. Images of mice treated with the control IgG (3207), MOR20350 and MOR20358 on day 29 as well as mice treated with MOR20350 on day 43 post-implantation are shown.

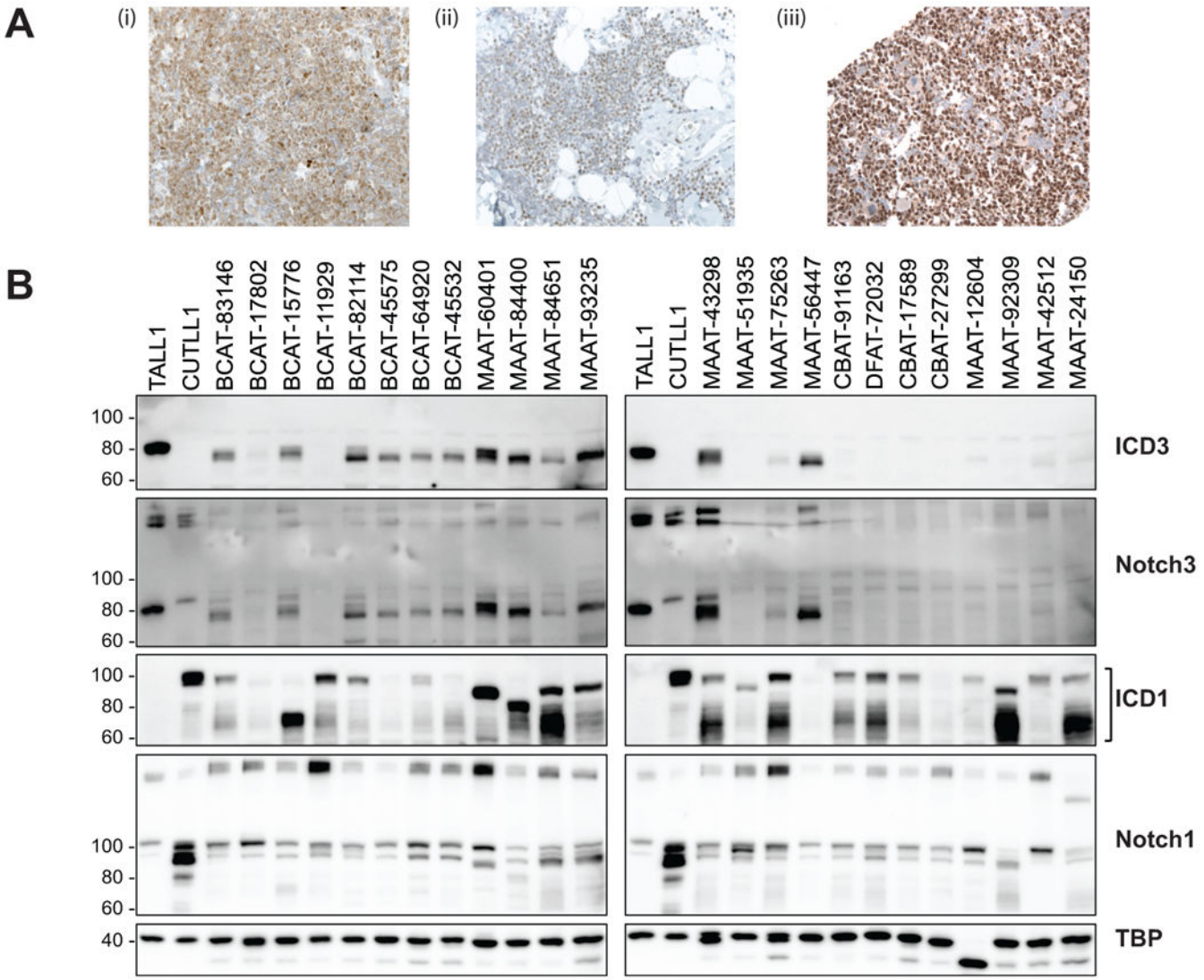

Figure 6. NOTCH3 signaling is activated in T-ALL patient samples

(A) ICD3 immunohistochemistry from 2 T-ALL patient samples (i and ii) and the TALL-1 cell line (iii). (B) 24 T-ALL PDX (patient derived xenograft) samples were analyzed for presence of total NOTCH3, ICD3, total NOTCH1and ICD1 protein by Western blotting. For total NOTCH3, the bands at ~80 kDa represent the TM-ICD or ICD3 while the bands at ~270 kDa represent the full-length NOTCH3. For total NOTCH1 the bands at ~100-120 kDa represent the TM-ICD or ICD1 while the bands at ~300 kDa represent the full-length NOTCH1 or furin processed NOTCH1. TALL-1 and CUTLL1 cell lysates were used as positive controls for ICD3 and ICD1 respectively.

Table 1
Binding properties of NOTCH3 antibodies

Antibody	Domain	FACS EC_{50} (nM)	K_D (nM)
MOR20350	NRR	0.16	0.3
MOR20337	NRR	0.34	0.4
MOR20358	NRR	0.14	0.6
MOR12229	LBD	s.n.r	11
MOR20364	LBD	0.1	0.1
MOR20802	LBD	0.01	n.d.

s.n.r saturation not reached

n.d. no data